

## Fluorinated diphenylalanine analogue based supergelators: a stencil that accentuates the sustained release of antineoplastic drugs

Priyanka Tiwari , Arindam Gupta , Radha Rani Mehra , Naureen Khan , Jeena Harjit , Charles R. Ashby Jr. , Anindya Basu , Amit K. Tiwari , Manju Singh & Anita Dutt Konar

To cite this article: Priyanka Tiwari , Arindam Gupta , Radha Rani Mehra , Naureen Khan , Jeena Harjit , Charles R. Ashby Jr. , Anindya Basu , Amit K. Tiwari , Manju Singh & Anita Dutt Konar (2020): Fluorinated diphenylalanine analogue based supergelators: a stencil that accentuates the sustained release of antineoplastic drugs, *Supramolecular Chemistry*, DOI: [10.1080/10610278.2020.1808892](https://doi.org/10.1080/10610278.2020.1808892)

To link to this article: <https://doi.org/10.1080/10610278.2020.1808892>



Published online: 30 Aug 2020.



Submit your article to this journal [↗](#)



Article views: 5



View related articles [↗](#)



View Crossmark data [↗](#)

ARTICLE



## Fluorinated diphenylalanine analogue based supergelators: a stencil that accentuates the sustained release of antineoplastic drugs

Priyanka Tiwari<sup>a</sup>, Arindam Gupta<sup>b</sup>, Radha Rani Mehra<sup>a</sup>, Naureen Khan<sup>a</sup>, Jeena Harjit<sup>c</sup>, Charles R. Ashby Jr.<sup>d</sup>, Anindya Basu<sup>e</sup>, Amit K. Tiwari<sup>f</sup>, Manju Singh<sup>a</sup> and Anita Dutt Konar<sup>a,e</sup>

<sup>a</sup>Department of Applied Chemistry, Rajiv Gandhi Proudyogiki Vishwavidyalaya, Bhopal, India; <sup>b</sup>Department of Chemistry, IISER, Bhopal, India; <sup>c</sup>Department of Applied Chemistry, Truba College, Bhopal, India; <sup>d</sup>St. Johns University, USA; <sup>e</sup>School of Pharmaceutical Sciences, Rajiv Gandhi Proudyogiki Vishwavidyalaya, Bhopal, India; <sup>f</sup>Department of Pharmacology and Experimental Therapeutics College of Pharmacy and Pharmaceutical Sciences, University of Toledo, Toledo, OH, USA

### ABSTRACT

Inspired by the prolonged metabolism displayed by para substituted fluorinated drugs, we intended to design two isomers Fmoc-(4F)-Phe-Phe-OH (hydrogelator I) & Fmoc-(3F)-Phe-Phe-OH (hydrogelator II) to explore the propensity of fluorine substitution in the aromatic ring of phenylalanine, in assisting or disrupting the gelation phenomena. However, our experimental observation reveals that hydrogelator I and II containing fluorines in the aromatic core illustrates excellent hydrogelation ability in comparison to the unsubstituted analogue, in accordance with the computational findings. Indeed, the hydrogelators displayed *b*-sheet with a fibrillar tape like morphology and were found to be biocompatible. We developed hydrogel nanoparticles (HNPs) that exhibited particle size less than 200 nm, and were found to release the antineoplastic drugs, 5Fluorouracil, curcumin and doxorubicin in a sustained manner depending on the architectural parameters of the drugs. Thus the prospective use of these compounds holds immense promise as a potential tool for future drug delivery applications.

### ARTICLE HISTORY

Received 20 July 2020  
Accepted 6 August 2020

### KEYWORDS

Hydrogel nanoparticles; high mechanical integrity; biocompatible; efficient drug delivery vehicle

## Introduction

The intrinsic behaviour of low molecular weight peptide-based hydrogels has gained significant impetus not only due to their interests in fundamental science but also their immense potential in biomedical applications [1–5]. Peptide-based hydrogels have a decreased capacity to produce environmental harm, that makes them appealing synthons for the design and development of soft materials [6]. Furthermore, they can self-assemble via the involvement of non-covalent interactions unlike other cross-linked polymers, that requires the presence of strong covalent linkages for its formation [7–15]. The fibrillar constructs that result from the hierarchical process of self-assembly, in three dimensions, develops large internal cavities, which entraps water molecules inside them, ultimately, leading to the formation of self-supporting hydrogels [16]. By simply changing the amino acid residues, one can fine-tune the properties and subsequently the mechanical strength of the hydrogels [16]. Although there are no definitive guidelines to design hydrogelators, the molecules that fail to form gels might provide better insights about the structural aspects of the synthons with high hydrogelation propensities [16].

Fluorine (F<sub>2</sub>), the first member of the halogen family, is a very rare element. Due to its prevalence in diverse molecular scaffolds, has been an area of significant interest [17–20]. Fluorine's high electronegativity, small atomic radius and strong C–F bond strength produce significant changes in various molecules [21]. However, investigations from proteins crystallographic database provided preliminary data regarding the interaction of fluorinated drugs with specific proteins [22]. In biomedical applications, F<sup>18</sup> isotope of fluorine have been routinely used in radiolabeling of biomolecules that served as a diagnostic probe for brain-imaging [23]. Even man-made fluorinated compounds have served noteworthy in various environmental concerns [24]. To date, fluorine biology has been focussed as one of the aspects of cutting-edge technologies [25–27]. Also, fluorine incorporation leads to reduced tooth decay [25–27]. The metabolism of certain drugs can be decreased by the presence of fluorine due to the high stability of the C–F bond [27]. Consequently, the drug is present in the blood for a longer period of time and thus the half-life is increased [27]. Furthermore, the presence of fluorine in drugs enhances the bioavailability due to increased cell membrane penetration as a result of the enhanced

hydrophobicity of C-F bond compared to C-H [28]. A recent study has shown how positional isomerism of fluorine in the aromatic ring produces supramolecular heterogeneity in peptidomimetic molecules [29,30]. Currently, there are only a few studies that have determined the effect of fluorine on supramolecular hydrogelation and the use of such molecules as efficient drug delivery modalities [31–33].

Ideally, an effective drug carrier should be a user-friendly delivery system comprising a scaffold with significant mechanical integrity and biocompatibility. It should deliver the drug to the area of therapeutic interest at a concentration that produces efficacy without exerting adverse toxic effects in the system, and get rapidly removed from the bloodstream in a secured pathway, without hampering normal body functioning.

In this regard peptide-based hydrogel nanoparticles have gained significant impetus in the last few decades in the area of drug delivery because of the following reasons: a) these particles possess small size and enhanced surface area, that increases the solubility and bioavailability, conferring them the ability to cross the blood–brain barrier (BBB) and be absorbed through the tight junctions of endothelial cells of the skin; b) their simple route of administration by direct injection [34]. One disadvantage associated with these particles is their hydrophobic nature that easily removes them from the bloodstream. Therefore, in this study, we sought to: a) design and synthesise biocompatible fluorine – substituted diphenylalanine derivatives that have a high hydrogelation potential and significant mechanical strength; b) develop an easy to use hydrophilic delivery system that would remain in the bloodstream for a prolonged period and c) determine the release profile of the antineoplastic drugs, namely 5-FU, doxorubicin and curcumin from the hydrogel matrix. Thus to meet our goal, we designed and synthesised two fluorinated phenylalanine derivatives, fluorenylmethoxy carbonyl (Fmoc)-(4 F)-Phe-Phe-OH

(hydrogelator I) and Fmoc-(3 F)-Phe-Phe-OH (hydrogelator II), by coupling 4/3-fluorinated phenylalanine and phenylalanine residues. To form a hydrophilic drug delivery system, we decided to coat the nanoparticles with the surfactant vitamin E-TPGS, such that they remain in the body environment for a prolonged period [34]. Our systematic approach in designing and testing the novel drug delivery system (DDS) hydrogel nanoparticles from fluorinated peptides have been discussed in detail in the subsequent sections (Figure 1).

## Experiment

### Materials and Methods

Fluorenylmethoxy carbonyl (Fmoc) chlorides, 5FU, curcumin, amino acids and other common chemicals/solvents used in the study were purchased from Spectrochem India. The surfactant vitamin-E-TPGS and doxorubicin were procured from Sigma Aldrich USA.  $^1\text{H}$  NMR spectra were recorded using a Bruker Ultra shield (400 MHz). Mass was measured using (ESI-MS mode) with a Micro TOF – Q-II instrument, IR with a Shimadzu, Prestige 21 FT-IR spectrometer and elemental analysis using CHN Analyser (Elementar, Germany).

### Synthesis of hydrogelator I and II

The hydrogelators were prepared using the solution phase methodology, where dicyclo-hexylcarbodiimide (DCC)/(1-hydroxybenzotriazole HOBt) was used as a coupling agent (Scheme 1) [35,36]. Methyl ester hydrochlorides of phenylalanine were synthesised utilising the thionyl chloride–methanol procedure [37,38]. The final derivatives were purified by column chromatography and the obtained derivatives were characterised by various analytical techniques as described.

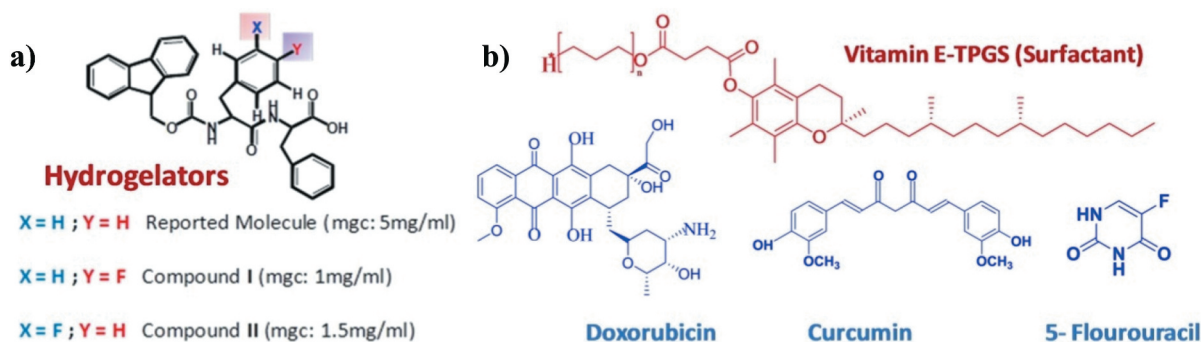
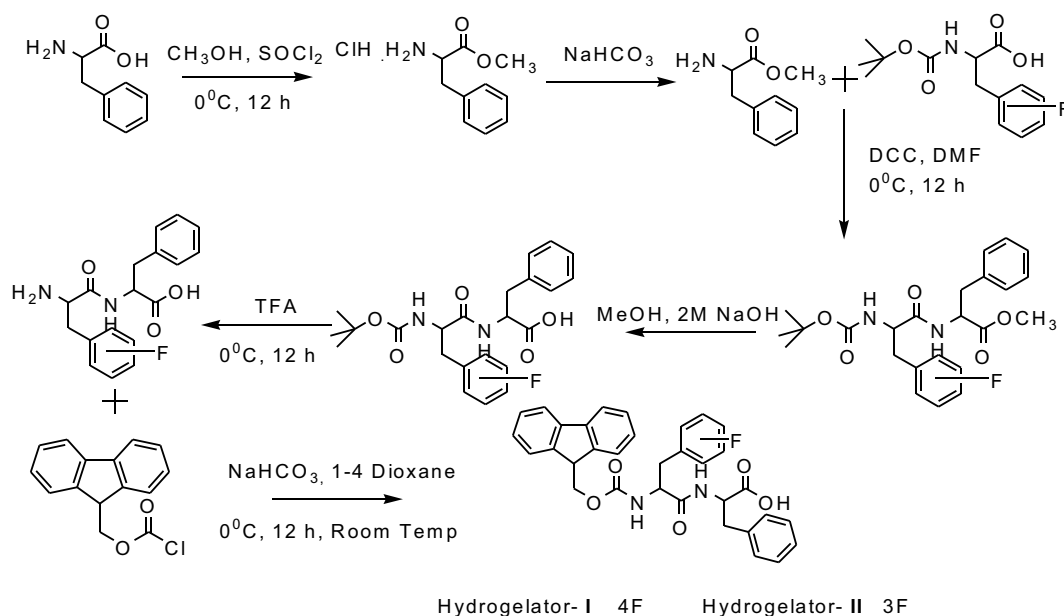


**Figure 1.** A) Schematic representation of the fluorinated hydrogelators; B) Other components involved in inverse emulsion technique, for the synthesis of HNPs.



**Scheme 1.** Synthetic Strategy of the hydrogelators, employing conventional solution phase methodology.

### Boc-(4 F)-Phe-Phe-OMe (1)

The free base of Phe-OMe obtained from its hydrochloride (5.34 g, 26.48 mmol) was poured into an ice-cold solution of Boc-4(F)Phe-OH (3 g, 10.59 mmol) in 10 ml of DMF, followed by DCC (3.27 gm, 15.88 mmol). The reaction mixture was stirred for 18 hours at room temperature. Subsequently, the mixture was filtered and taken up in ethyl acetate. The organic layer was washed with 2 M HCl solution, saturated sodium carbonate and a brine solution and then dried over anhydrous sodium sulphate and evaporated *in vacuo* to obtain a white solid.

Yield: 4.04 g (86%, 9.09 mmol).

### Boc-(4 F)-Phe-Phe-OH (2)

To a methanolic solution of compound **1** (4.04 g, 9.09 mmol), 2 N NaOH (3.5 ml) was added dropwise. The progress of the reaction was monitored using TLC. After completion of the reaction, the methanol was evaporated and the residue was dissolved in water and washed with diethylether. The aqueous layer was then acidified with 2 N HCl and extracted with ethyl acetate to obtain a white solid.

Yield: 3.40 g (87%, 7.89 mmol).

### Hydrogelator I

To an ice-cooled solution of (**2**) (3.40 g, 7.89 mmol) in DCM, trifluoroacetic acid (5 ml) was added and stirred until the Boc group was completely removed (based on TLC results). Next, trifluoroacetic acid was removed under reduced pressure to afford the crude trifluoroacetate salt. This dipeptide was dissolved separately in

sodium carbonate solution (basic, 17 ml) and further cooled in an ice-water bath. A solution of Fmoc-Cl (2.81 g), solubilised in dioxane (18 ml) was added to the cooled mixture from above and was stirred for 24 h. Finally, the pH was adjusted to an acidic level with concentrated HCl and extracted with ethylacetate. The organic layer was evaporated to get a white solid.

Yield: 3.43 g (85%, 6.22 mmol); M.p. 113–115°C, LC-MS:  $C_{33}H_{29}FN_2O_5$ ; m/z: 552.21  $[M]^+$  (calculated); m/z: 552.8  $[M]^+$  (obtained); FT-IR: 1442, 1566, 1648, 3232, 3230, 3406, 3482,  $cm^{-1}$ ;  $^1H$  NMR ( $d_6$ -DMSO, ppm, 25°C, 400 MHz): 3.70–3.75 ( $C^{\beta}Hs$  of 4 F-Phe (1), Phe (2) & Fluoren, 6 H, m), 3.96–3.99 (CH of Fluoren, 1H, m), 5.06–5.08 ( $C^{\alpha}Hs$  of 4 F-Phe (1), & Phe (2), 2 H, m), 7.26–7.38 (Aromatic protons of Fluoren, Phe (2) & NH of 4 F-Phe (1), & Phe (2), 15 H, m), 7.66 (Aromatic protons of 4 F-Phe (1), 2 H, d,  $J = 8$  Hz), 7.83 (Aromatic protons of 4 F-Phe (1), 2 H, d,  $J = 8$  Hz).  $^{13}C$  NMR (100 MHz,  $d_6$ -DMSO, 25°C, 400 MHz): 161.357, 161.190, 154.833, 150.97, 150.874, 145.681, 143.722, 141.264, 141.068, 128.248, 127.679, 127.190, 125.746, 125.361, 124.416, 120.716, 120.278, 69.153, 64.259, 50.564, 46.659; Anal. Calcd for  $C_{33}H_{29}FN_2O_5$  (552.59): C, 71.72%; H, 5.28%; N, 5.07%. Found: C, 71.70%; H, 5.13%; N, 4.88.

### Hydrogelator II

Hydrogelator **II** was prepared using the same synthetic procedure as that of Hydrogelator **I**. Yield: 3.51 g (87%, 6.36 mmol); M.p. 110–113°C, LC-MS:  $C_{33}H_{29}FN_2O_5$ ; m/z: 552.21 (calculated); m/z: 580.8  $[M^+ Na^+ 5 H]^+$  (obtained); FT-IR: 1418, 1538, 1622, 3250, 3426, 3488, 3564,  $cm^{-1}$ ;  $^1H$  NMR ( $d_6$ -DMSO, ppm, 25°C): 3.71–3.73 ( $C^{\beta}Hs$  of

4 F-Phe (1) & Phe (2), 4 H, m), 3.96–3.99 ( $C^{\beta}$ Hs of Fluoren, 2 H, m), 4.22–4.26 (CH of Fluoren, 1H, m), 4.46–4.48 ( $C^{\alpha}$ Hs of 4 F-Phe (1), & Phe (2), 2 H, m), 7.26–7.88 (Aromatic protons of Fluoren, 4 F-Phe (1), Phe (2) & NH of 4 F-Phe (1), & Phe (2), 19 H, m);).  $^{13}C$  NMR (100 MHz,  $d_6$ -DMSO, 25°C, 400 MHz): 161.312, 154.833, 145.462, 143.871, 128.189, 127.768, 127.679, 127.555, 127.313, 127.190, 125.733, 125.259, 124.416, 120.667, 120.389, 119.480, 69.200, 64.259, 50.564, 46.635; Anal. Calcd for  $C_{33}H_{29}FN_2O_5$  (552.59): C, 71.722; H, 5.289; N, 5.07. Found: C, 71.502; H, 5.126; N, 4.74.

### Computation calculations

The molecules were modelled using Spartan08 software and energy minimisation was done there itself. Calculations were done on a single molecule. Further, optimisation and frequency calculation with tight convergence criteria was done on the obtained minimised structure in Gaussian 09 software package using B3LYP functional and 6–31 G basis set. Molecular Orbital calculations were performed on these optimised structures. HOMO-LUMO diagrams of the Hydrogelators were generated using GaussView 5.0 [39].

### MTT assay

The cytotoxicity of hydrogelator-I was determined through MTT (methyl thiazolyl tetrazolium) colourimetric assay, which measures cell metabolic activity through the conversion of tetrazolium dye to insoluble purple formazan crystals as per the method described [40–42]. The dipeptides were dissolved in DMSO stock solutions followed by making the dilutions (with DMSO 0.01%) directly using cell culture media. No precipitation or aggregates were observed even on storage up to 72 h at 37°C. The cells were seeded onto flat-bottom 96 well plates at a density of 4000–5000 cells per well. After 24 h, the cells were drugged with serial dilutions (0, 0.1, 0.3, 1, 3, 10, 30, 100 mM) for each of the compounds in triplicate. After 72 h of incubation, MTT dye (4 mg) was added to all wells and incubated at 37°C for an additional 4 h. The medium was carefully discarded after this incubation period and formazan crystals were dissolved in 100  $\mu$ l of DMSO in each well for 15 minutes. Absorbance was measured at a wavelength of 570 nm using a DTX 880 multimode detector (Beckman Coulter Life, Indianapolis, IN, USA). The raw data were analysed and plotted using GraphPad Prism7.02. Student's t-test was used to analyse all the data [40–42].

## Results and discussion

### Design and characterisation of the hydrogelators

Certain aromatic compounds can be biotransformed into toxic epoxides specific drug metabolising enzymes, by the body's native enzymes [27]. Substituting a fluorine into the *para* position of the aromatic ring, however, restricts this process [27]. Inspired by this event, with the aim of construction of novel hydrogels, we decided to substitute the *para* position of first ring of N-terminally protected diphenylalanine, Fmoc-(4 H)-Phe-Phe-OH (Reported Molecule) by Fmoc-(4 F)-Phe-Phe-OH (hydrogelator I), to determine the effect of fluorine substitution in inducing gelation phenomena (Figure 1).<sup>43</sup> To further decipher the outcome of positional isomerism on self-assembly we synthesised Fmoc-(3 F)-Phe-Phe-OH (hydrogelator II). The diphenylalanine fragment was chosen due to its high hydrogel-forming ability [43]. The Fmoc group was introduced to promote self-assembly by its increased  $\pi - \pi$  correspondence.

Interestingly, both hydrogelator I and II had excellent hydrogel-forming capacity at room temperature, with an mgc of 0.01% and 0.015% w/v, respectively. To confirm this property, the hydrogelators were initially dissolved in 1 ml of water under mild heating conditions and allowed to cool. The solvent system was almost instantaneously immobilised into a translucent mass, confirming the formation of gels.

Next, we determined the stability of the gels by investigating the sol – gel interconversion temperatures (T<sub>gel</sub>) at different hydrogelator concentrations (Figure 2). Importantly, the generated curves indicated an increase of the T<sub>gel</sub> value up to the saturation limit. Moreover, we postulated that the self-assembly process

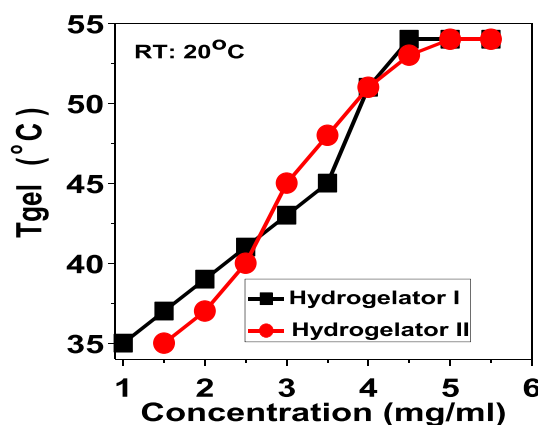


Figure 2. T<sub>gel</sub> curves as a function of hydrogelator concentration.

is regulated by intermolecular non-covalent interactions, which might have been optimal at the saturation limit. Indeed, it has been reported that at the level of saturation, an increase in the hydrogelator concentration did not significantly alter the  $T_{gel}$  (temperature) [12,13,40–42].

Generally, gelators with mgcs below 0.1% (w/v) are categorised as supergelators [11]. Therefore, our mgc values allowed us to characterise our hydrogelators as supergelators. Our results are consistent with those of Mahler *et al.* who reported that the unsubstituted analogue, Fmoc-Phe-Phe-OH, had an mgc of 0.05% w/v in water [43]. However, our fluorinated derivatives had mgcs lower than 0.05% (Hydrogelator I: 0.01% and Hydrogelator II: 0.015% w/v). Therefore, our initial experiments suggested that fluorination accentuates the process of hydrogelation.

### Computation investigation about the effect of fluorine substitution in diphenylalanine in hydrogelation

To search an explanation for the above observation, we performed computational analysis using Gaussian09 software package with B3LYP functional and 6–31 G basis set [39]. Figure 3 shows that introduction of Fluorine seems to have considerable impact on the HOMO/LUMO energies of the molecules, owing to subtle changes in the electronic distribution of the system (Table 1). For example, unlike the unsubstituted analogue ( $\log P = 2.36$ ), Hydrogelators I and II are more

hydrophilic ( $\log P = 1.76$ ). Also, the substitution of a fluorine atom at the para position significantly changes the electrostatic charge distribution compared to the meta derivative, which could account for the difference in threshold concentration with respect to the unsubstituted derivative (Figure 3, Table 1). Additionally, we observe that the final potential energy and zero point vibrational energy of the fluorinated derivatives are lower in comparison to the unsubstituted one. This makes both of their summation even lower (Table 1). Overall, based on the results of the experimental and computation studies, we postulate that the fluorine introduction not only enhances the hydrophilic–lipophilic balance but also gives rise to the possibilities of new electrostatic interactions, thereby providing the opportunity to obtain better hydrogels.

### Determination of the mechanical strength, morphology and conformation of the hydrogelators

Firstly, we determined the mechanical integrity of the hydrogelators by performing rheological measurements with freshly prepared hydrogels of concentration 2 mg/ml. As shown in Figure 4, throughout the viscoelastic region, the storage modulus ( $G'$ ), the loss modulus ( $G''$ ) (Figure 4(a)), and the complex viscosity (Figure 4(b)) were determined as a function of angular frequency. The results indicated the formation of a soft gel phase [11–13]. We then performed an amplitude sweep measurement, where the strain was varied to 100%. We noticed in the lower viscosity region, the  $G'$  was higher

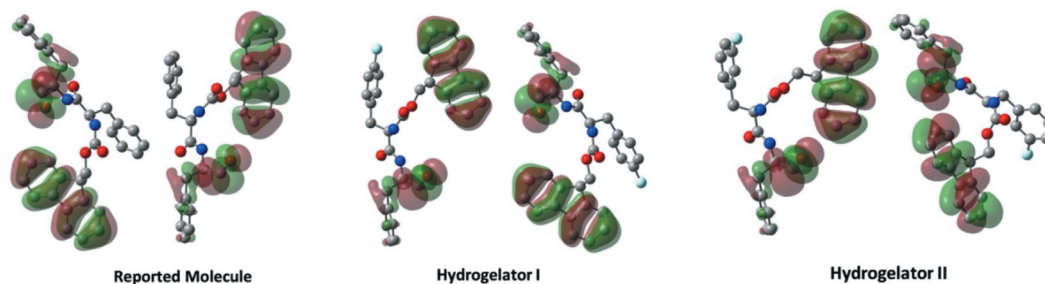
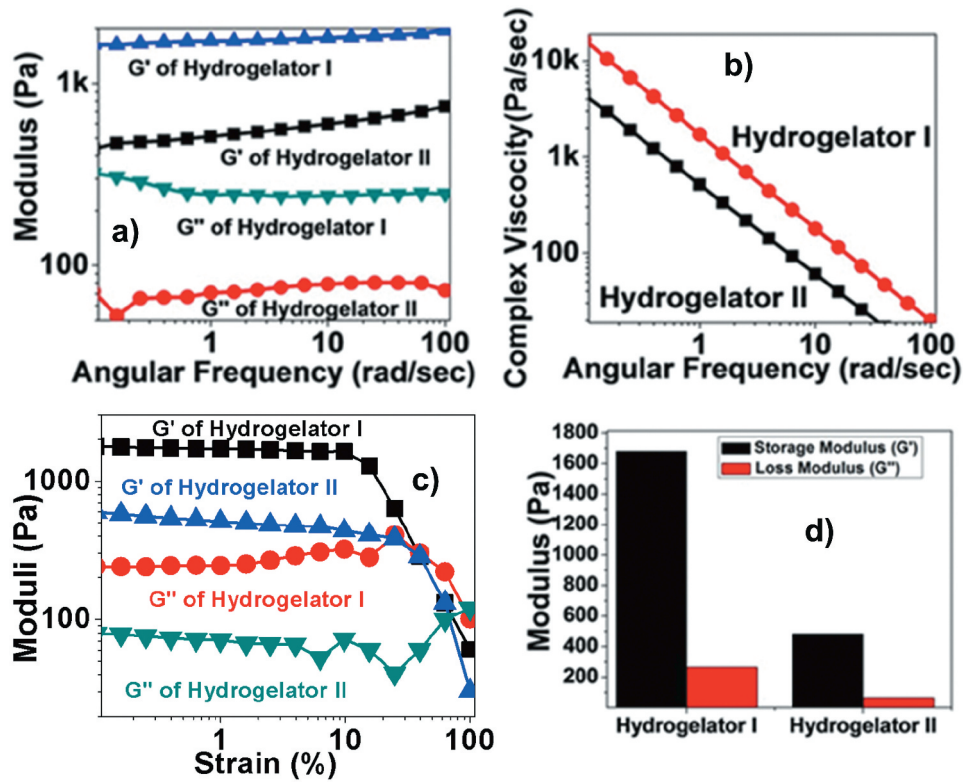


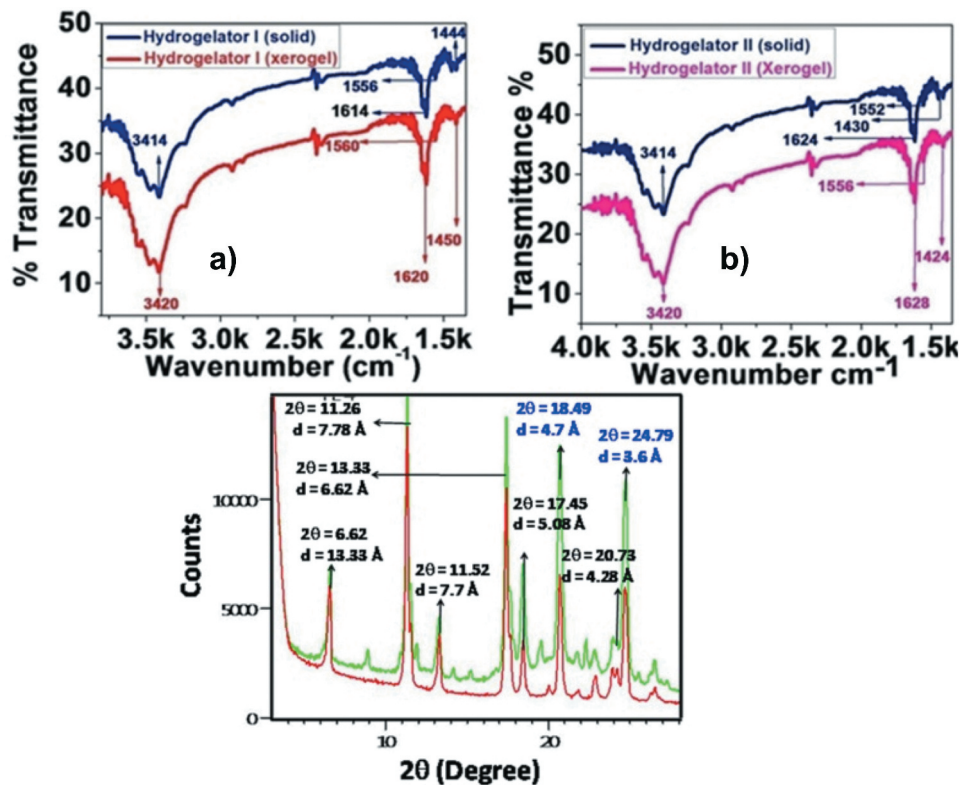
Figure 3. HOMO-LUMO Orbitals of I) reported molecule II) hydrogelator I and III) II.

Table 1. Experimental parameters of the underivatized and derivatized fluorine analogues probable constructs responsible for driving the gelation mechanism.

| Hydrogelators | HOMO      | LUMO      | Final Energy | Zero-point vibrational energy: | Sum of thermal and vibrational Enthalpy |
|---------------|-----------|-----------|--------------|--------------------------------|-----------------------------------------|
| Unsubstituted | -5.897 eV | -1.5 eV   | -1685.586    | 355.871                        | -1684.984                               |
| I             | -5.842 eV | -1.597 eV | -1784.800    | 350.758                        | -1784.206                               |
| II            | -5.784 eV | -1.697 eV | -1784.801    | 350.683                        | -1784.207                               |



**Figure 4.** Frequency sweep of A) Dynamic Shear Modulus; B) Complex Viscosity; C) Amplitude sweep of the hydrogels made from hydrogelator I and II at 2 mg/ml concentration at room temperature. D) Bar graph representation of the comparison of the elastic response ( $G'$ ) and viscous response ( $G''$ ) of the hydrogelators.



**Figure 5.** FT-IR and PXRD spectra of the Hydrogelators showing  $\beta$ -sheet-like conformation. The characteristic peaks in the PXRD curve are presented in blue.

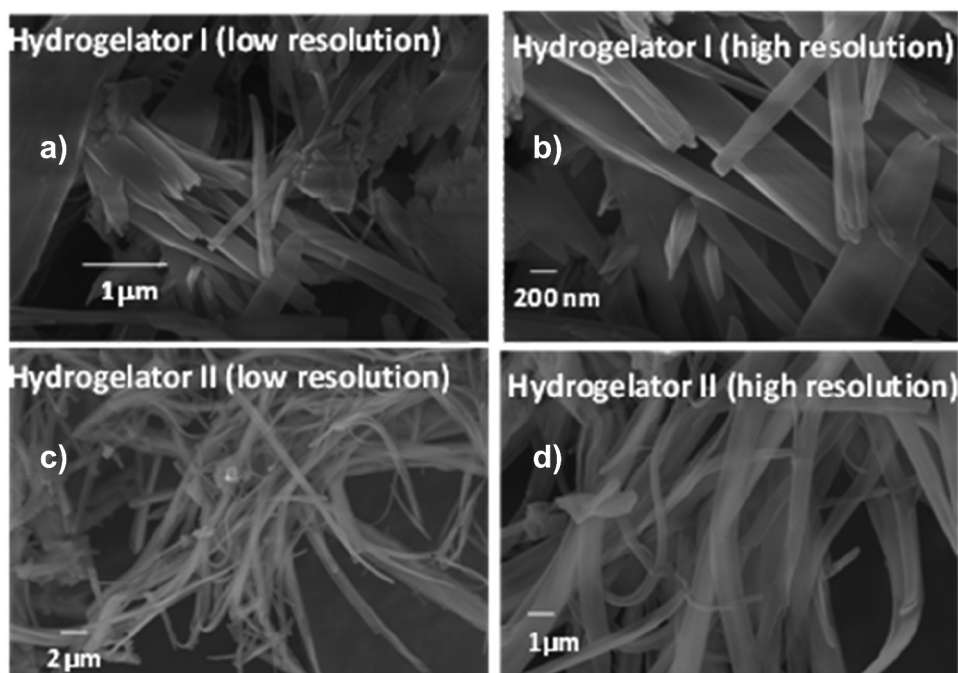


**Figure 6.** FE-SEM images of hydrogelator **I** and **II**, (A, C: low resolution; B, D: high resolution) showing the formation of three-dimensional dense fibrillar network. The remaining sol was, immobilised within the cavities of the network, thereby forming self-supporting hydrogels.

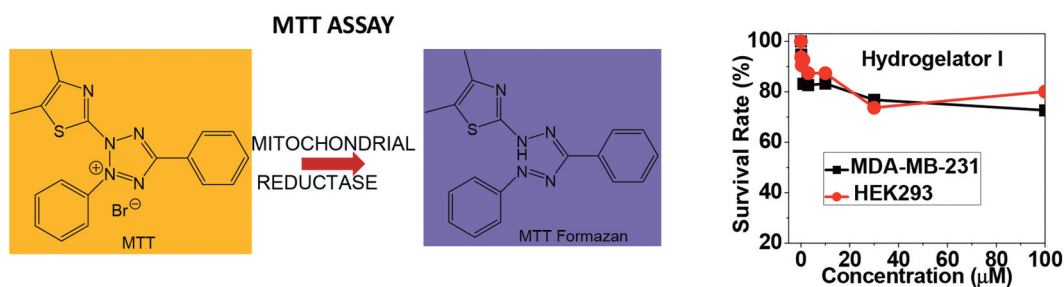


**Figure 7.** Basic Principle of MTT Assay (Top); Biocompatibility Studies of Hydrogelator **I** in two different cell lines MDA-MB-231 and HEK 293 (Bottom).

than the  $G''$ , indicating the stabilisation of the gel phase. But the sooner, the strain reached to 39.6% and 63% for hydrogelators **I** and **II** respectively, a cross over point was observed in the experimental frequency region, where the value of loss modulus  $G''$  slightly exceeds the value of storage modulus  $G'$  and transformed into solution state (Figure 4(c)). This particular point where the crossover occurs is called yield stress ( $\sigma_y$ ). These soft materials displayed the gelation property until the threshold value of strain is reached which is 39.6% and 63% for hydrogelators **I** and **II** respectively (Figure 4(c)). As the strain was increased beyond this threshold, the intermolecular forces that held the gel together started being overcome by the applied strain and the xerogel

fibrils were unable to withstand deformations. The frequency-sweep experiments further showed that both the  $G'$  and  $G''$  values were weakly dependent on the frequency which was indicative of an entangled network-like system.

Also, the moduli remained parallel to the x-axis, indicating that the obtained hydrogels were stable and rigid (Figure 4(a-b)). The data further confirmed that Hydrogelator **I** ( $G'$ : 1700 Pa) had a higher gel strength compared to Hydrogelator **II** (500 Pa) for gels of same concentration, emphasising the importance of position of fluorine in regulating mechanical integrity (Figure 4(d)).

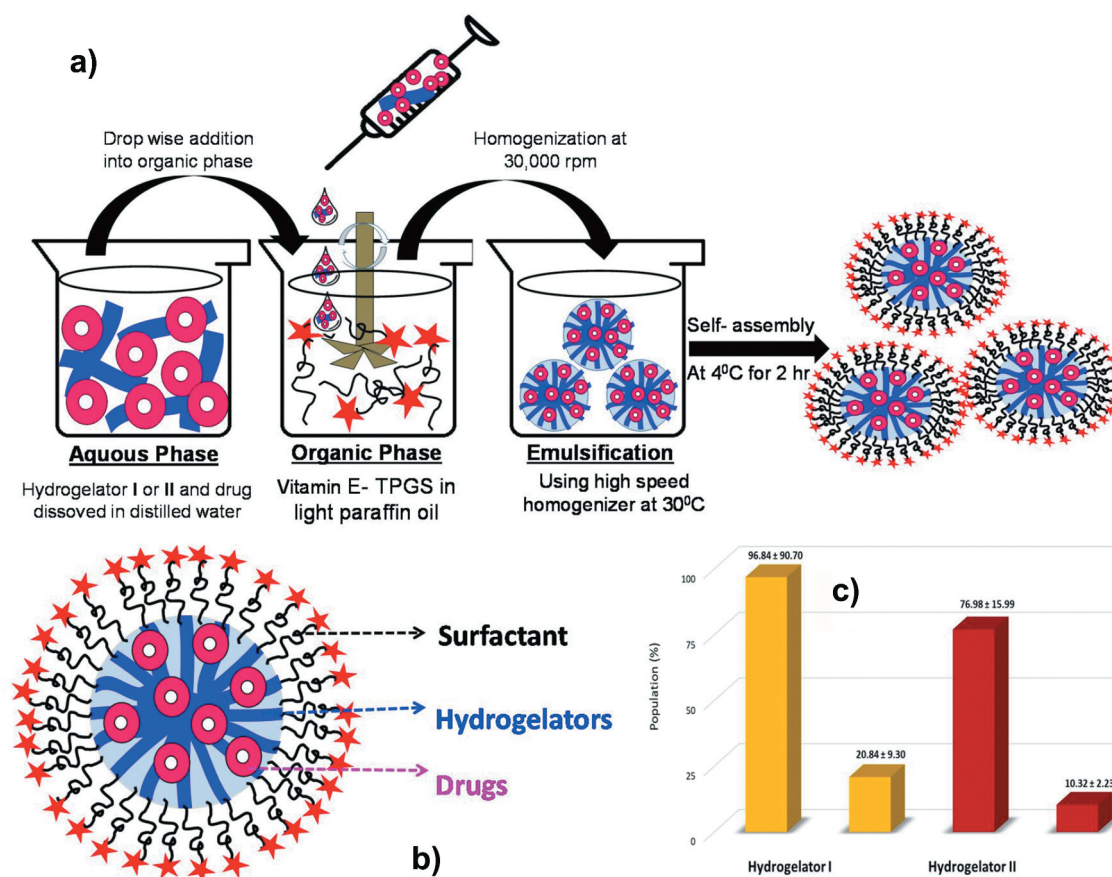


**Figure 8.** A) Inverse Emulsion Technique; B) Enlarged cartoon Diagram of Hydrogel Nanoparticle; C) Particle Size Dimension of the HNPs.

**Table 2.** Comparative study of particle dimension/release time and percentage of various drugs from the HNPs developed from Hydrogelators I and II.

| Hydrogelators | Particle Size (nm)            | Time of release of 5FU | % of 5-FU released                      | Time of release of Doxorubicin | % of Doxorubicin released               | Time of release of Curcumin | % of Curcumin released | Ref  |
|---------------|-------------------------------|------------------------|-----------------------------------------|--------------------------------|-----------------------------------------|-----------------------------|------------------------|------|
| Unsubstituted | 225.9 ± 3.6<br>21.5 ± 0.1     | 5 h                    | 50%                                     | 20 h                           | 50%                                     | ---                         | -----                  | 48   |
| <b>I</b>      | 96.84 ± 90.70<br>20.84 ± 9.30 | 50 h                   | 30%                                     | 112 h                          | 30%                                     | 70 h                        | 30%                    | This |
| work          | Control (only gel)            | 9 h                    | 50% followed by immediate burst release | 22 h                           | 50% followed by immediate burst release | ---                         | -----                  | This |
| <b>II</b>     | 76.98 ± 15.99<br>10.32 ± 2.23 | 50 h                   | 30%                                     | 72 h                           | 30%                                     | 88 h                        | 30%                    | This |
| work          | Control (only gel)            | 9 h                    | 50% followed by immediate burst release | 22 h                           | 50% followed by immediate burst release | ---                         | -----                  | This |
| work          |                               |                        |                                         |                                |                                         |                             |                        |      |

In order to determine the origin of the mechanical strength, we performed structural studies using Fourier Transform–Infra Red Spectroscopy and PXRD Analysis. Figure 5(a-b) shows the overlapped FTIR spectra from

the solid sample as synthesised and the xerogels, respectively. Each molecule of the Hydrogelators contained two NH protons and three carbonyl moieties (Figure 1).

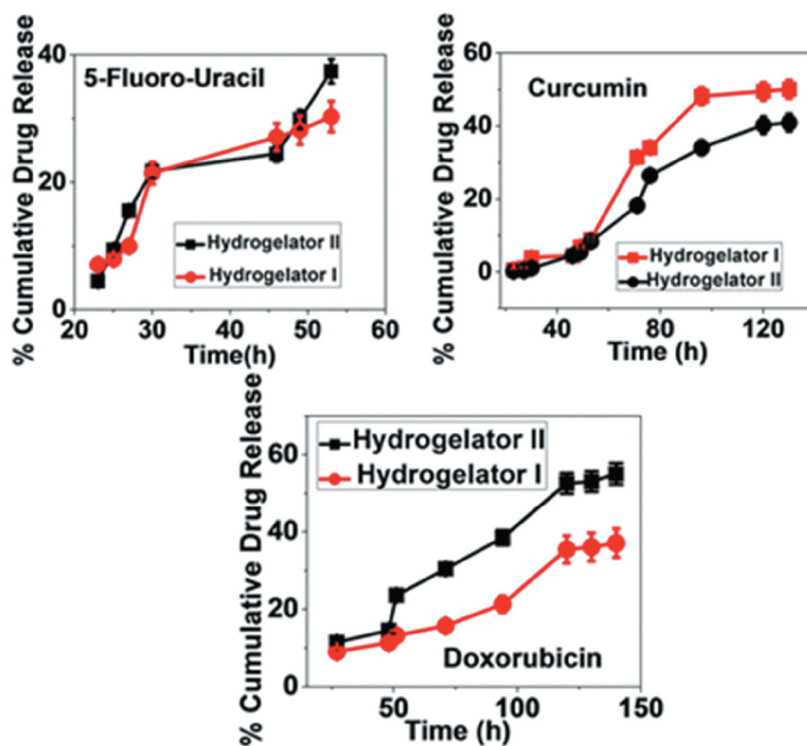


Figure 9. % Cumulative drug release profile of the three antineoplastic drugs from the hydrogel matrix.

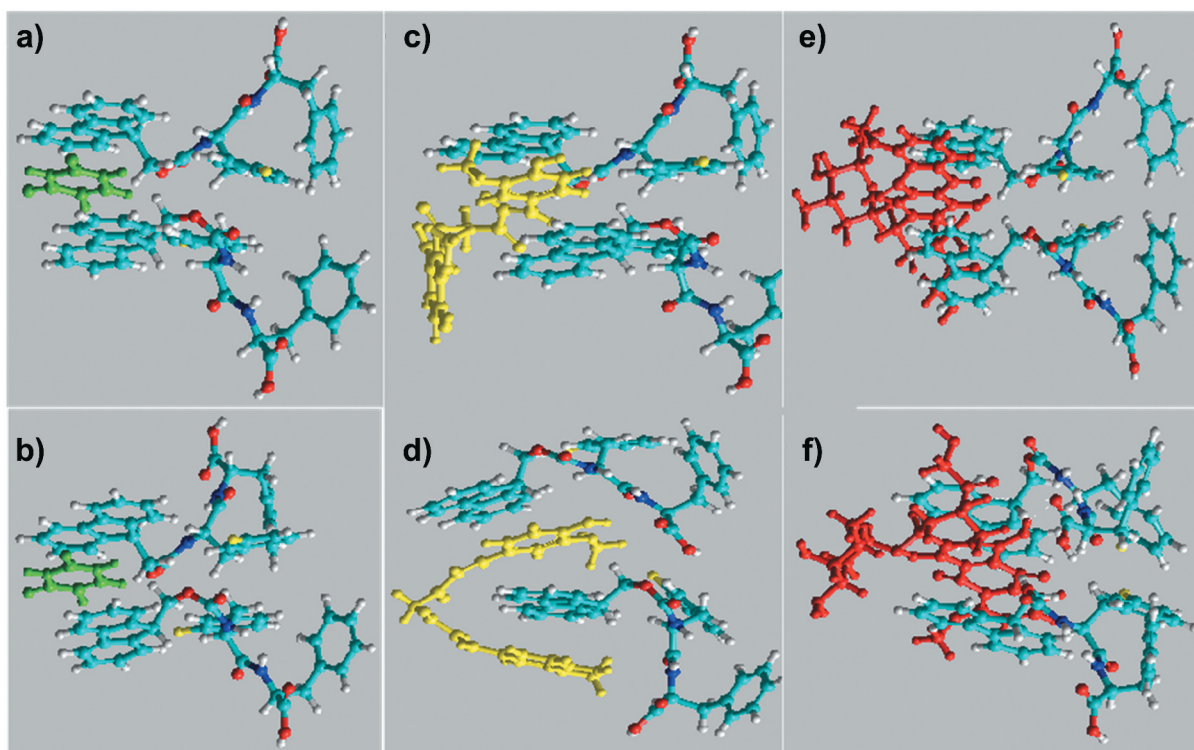


Figure 10. Computation investigation of hydrogelator -drug interactions. The model drugs that have been used are 5Fluorouracil (green), Curcumin (yellow) and Doxorubicin (red). Interactions of 5-FU/Curcumin/Doxorubicin with A/C/D) Hydrogelator I and B/D/F) Hydrogelator II.

The peaks for the NH protons in both states appeared at 3390/3330  $\text{cm}^{-1}$  for Hydrogelator **I** and **II**. These data indicated that the NHs were H-bonded in Hydrogelator **I** and **II**. In contrast, the amide I and II carbonyl had characteristic peaks at 1620/1528/1464  $\text{cm}^{-1}$  for Hydrogelator **I** and 1612/1556/1448  $\text{cm}^{-1}$  for Hydrogelator **II**, respectively (Figure 5).

A closer analysis of the spectra further showed that although the peak characteristic remained the same in both states, the peaks were slightly broadened and shifted for both the Hydrogelators. This could only occur when the non-covalent interactions, namely H-bonding and Van der Waals interactions form fibrous network in three dimensions, that could immobilise the remaining sol in them and form gels. Overall, the FT-IR data were indicative of the dominant role of  $\beta$ -sheets in the respective xerogel state [11–13,44,45].

To re-confirm our investigations we performed PXRD experiments with the xerogels of the hydrogelators [40–42]. The wide-angle PXRD curves showed apparently similar patterns, with periodic diffractions, common in both the hydrogelators. This data indicated the presence of ordered structures in the xerogels. Additionally, the characteristic peaks at 18.49° ( $d = 4.9 \text{ \AA}$ ) might have arisen due to the presence of the  $\beta$ -sheet-like packing in the hydrogelators. We believe that this  $\beta$ -sheet formation could only be possible because of an effective overlap between the aromatic rings of Phenylalanine and Fmoc moiety, stabilised by  $\pi$ - $\pi$  interactions. Indeed, the peak at 24.79° ( $d = 3.7 \text{ \AA}$ ) further affirmed our analogy. Thus, taken together the result of FT-IR and PXRD data, our finding revealed the presence of  $\beta$ -sheet conformation in the xerogels [40,41]. To obtain additional data about the morphological arrangement of the xerogels, we conducted FE-SEM studies with the xerogels obtained from the corresponding hydrogels (the same concentration and magnification were used for both the hydrogelators) (Figure 6). The FE-SEM images showed the formation of dense, fibrillar tape-like structures that were approximately 500 nm in width and several micrometres in length. We postulated that these tapes were intertwined with one another, producing a three-dimensional network that served as a template to immobilise the remaining sol (water) and form self-supporting hydrogels. Since the hydrogelators bear isomeric relationship, they had a similar fibrillar network. However, the fibres in hydrogelator **I** were thick and more densely packed compared to hydrogelator **II**, thus accounting for the differences in mechanical strength and the minimum gelation concentrations. Also, the differences in the HOMO/LUMO energies, final potential energy and zero point vibrational energy

provide additional data, supporting the nature of fibrillar network (Table 1). Interestingly, the tenacity of hydrogelator **II** was more than that of **I**, as reflected from Figure 4(c) (cross over point was observed at 39.6% and 63% strain for hydrogelators **I** and **II**, respectively).

### *Biocompatibility studies*

Biocompatibility is an important characteristic for a molecule to be used as a delivery system, which is generally probed by MTT assay (Figure 7 top) [40–42]. Therefore, using this technique, we determined the effect of the hydrogelators on the viability of human embryonic kidney (HEK-293) and epithelial human breast cancer cells (MDA-MB-231, as shown in Figure 7 (bottom)). Since our hydrogelators are isomers, we conducted the experiment with only hydrogelator **I**, as isomers are known to have similar behaviour. The  $\text{IC}_{50}$  values of hydrogelator **I** were  $>100 \mu\text{M}$  for both cell lines, thereby allowing us to conclude the molecule to be biocompatible [11–13,40–42].

### *Why peptide-based hydrogel nanoparticles in drug delivery?*

In the last few decades, the development of nanoparticles from various polymers and its use in drug formulation have helped advance the treatment of certain diseases [46]. However, one of the major problems associated with various polymers is that they produce toxicity in normal cells.

Peptide – based hydrogel nanoparticles are less toxic as they consist of biocompatible amino acids. Indeed, from the literature, we confirmed that for therapeutic use, the preferred size of the nanoparticles should be less than 200 nm [47,48]. In the section below, we discuss the preparation of nanoparticles that contain fluorinated hydrogelators and determine their drug delivery efficiency.

### *Preparation of hydrogel nanoparticles and its release kinetics using anti-cancer drugs*

The hydrogel nanoparticles (HNPs) were synthesised using a modified inverse emulsion protocol as shown in Figure 8(a-b). The hydrogelators had a bimodal distribution of particle size, with a dimension  $96.84 \pm 21.32 \text{ nm}$  and  $20.84 \pm 3.25 \text{ nm}$  for hydrogelator **I** and  $76.98 \pm 15.99 \text{ nm}$  and  $10.32 \pm 2.23 \text{ nm}$  for hydrogelator **II** (Figure 8(c)). This bimodal particle size distribution is probably a result of equilibrium between droplet fragmentation and droplet re-coalescence that

occurs due to variation in experimental conditions [11,12,48]. Indeed, a higher value of negative zeta potential ( $-30$  mV, the value should be high irrespective of the charge) indicated the presence of system stability. This negative charge might be due to the presence of carboxylates, as well as the surfactant coating around the hydrophobic core [11,12]. Since the size of the particles were less than 200 nm, we hypothesised that our designed HNPS would release a greater percentage of the drugs compared to the reported analogue and control hydrogelators (normal hydrogel, without forming nanoparticles) for prolonged period of time (Table 2).

To test this hypothesis, we chose three different drugs: 5-FU, curcumin and doxorubicin, which had varying properties, structures (structures shown in Figure 7 (b)) and chemotherapeutic efficacy [11–13,40–42,49].

Figure 9 represents the release kinetics of the drugs over a stipulated period of time, which showed a marked difference with variation in their respective molecular weights. As evident from the figure, about 30% of the 5-FU content, from both hydrogelators were released after a 50-h incubation period. In contrast, it took 70 and 88 hours for the release of 30% of the curcumin content from Hydrogelator I and II, respectively. The release of 30% of the doxorubicin took 112 hours from the matrix of Hydrogelator I and 72 hours from that of Hydrogelator II.

To account for the differential behaviour in release mechanism, we performed computation analysis to investigate the interactions of the drugs with the hydrogelators.

As revealed from Figure 10, initially two molecules of the energy optimised hydrogelators could be imagined to be oriented in the form of a clip, such that Fmoc moieties lie on one end and Phe-Phe rings on the other. Now the 5-FU, containing 30% aromatic character, apart from H-bonding donors and acceptors, in order to maximise  $\pi$ - $\pi$  interactions with the Fmoc units, remains at the mouth of the clip [50]. So its release from the matrix of both the hydrogelators becomes easier and faster (Figure 10(a-b)). Although curcumin/doxorubicin possessed both H-bond donors and acceptors along with aromatic units, here the drug-matrix interaction occurs mainly by hydrophobic and  $\pi$ - $\pi$  interactions (Figure 10(c-d)). For curcumin, we observe that in case of hydrogelator II, the drug becomes sandwiched between the Fmoc moieties of the clip, in an organised fashion, stabilised by  $\pi$ - $\pi$  interactions, unlike hydrogelator I (sandwiched in a disordered manner), which might be the cause of its slower release from the hydrogel matrix. Again for Doxorubicin, we observe that for both the hydrogelators, the drug stabilises itself by entering deep into the pin pocket, utilising non-covalent

interactions. This stabilisation might be greater in case of hydrogelator I, than II. Henceforth, the release of the former gets drastically slowed (Figure 10(e-f)). Taken together these results, we attribute the entire mechanism of release pattern, to the variation in position of fluorine in the aromatic ring of diphenylalanine and physicochemical properties of the drugs. Actually, these two scaffolds (drug and hydrogelators) interact with each other in different extents, leading to overall stabilisation of the motifs, resulting in faster/delayed release response in different cases.

## Conclusions

In summary in this report, we have successfully designed and developed a set of fluorinated peptides that displayed excellent hydrogelation phenomena in aqueous medium.

Our experimental observations backed by computational calculations, additionally revealed that fluorine substitution in the aromatic ring in phenylalanine ring (hydrogelator I and II) definitely enhanced the gelation aptitude in comparison to the unsubstituted analogue. Indeed, the hydrogelators showed significant mechanical strength and biocompatibility, ample enough to be used for drug delivery applications. So we devised formulation to synthesise hydrogel nanoparticle with the biocompatible hydrogelators. We believe that mere linkage of vitamin E-TPGS at the surface could convert the nature of the nanoparticle from hydrophobic to hydrophilic, thereby increasing the blood retention time. Importantly the synthesised hydrogel nanoparticles exhibit particle size less than 200 nm, thereby accounting for their accentuated efficacy to release the antineoplastic drugs at physiological conditions. Overall this study illustrates that through fine-tuning the particle size and appropriate surface modification, we might be capable to develop better transport system efficient enough to deliver drugs for prolonged period with less frequent dosing (sustained release) along with greater precision and penetration in tissues difficult to access.

## Acknowledgments

PT and RRM acknowledge CSIR/UGC for research fellowships. ADK is grateful to UGC (F.4-(55)/2014(BSR)/FRP), New Delhi, and TEQIP 61, for financial support.

## Disclosure statement

The author declares no conflict of interest.

## Funding

This work was supported by the TEQIP, RGPV Bhopal, India [61]; University Grants Communication, New Delhi, India [F.4-(55)/2014(BSR)/FRP].

## References

- [1] Sun L, Zheng C, Webster TJ. Self-assembled peptide nanomaterials for biomedical applications: promises and pitfalls. *Int J Nanomedicine*. **2017**;12:73–86.
- [2] Schnaider L, Brahmachari S, Schmidt NW, et al. Self-assembling dipeptide antibacterial nanostructures with membrane disrupting activity. *Nat Commun*. **2017**;8:1365.
- [3] Collier JH, Rudra JS, Gasiorowski JZ, et al. Multi-component extracellular matrices based on peptide self-assembly. *Chem Soc Rev*. **2010**;39:3413–3424.
- [4] Segarra-Maset MD, Nebot VJ, Miravet JF, et al. Control of molecular gelation by chemical stimuli. *Chem Soc Rev*. **2013**;42:7086–7098.
- [5] Rutgeerts LAJ, Soultan AH, Subramani R, et al. Robust scalable synthesis of a bis-urea derivative forming thixotropic and cytocompatible supramolecular hydrogels. *Chem Commun*. **2019**;55:7323–7326.
- [6] Ulijn RV, Smith AM. Designing peptide based nanomaterials. *Chem Soc Rev*. **2008**;37:664–675.
- [7] Nandi N, Gayen K, Ghosh S, et al. Amphiphilic peptide-based supramolecular, noncytotoxic, stimuli-responsive hydrogels with antibacterial activity. *Biomacromolecules*. **2017**;18:3621–3629.
- [8] Basu K, Baral A, Basak S, et al. Peptide based hydrogels for cancer drug release: modulation of stiffness, drug release and proteolytic stability of hydrogels by incorporating D-amino acid residue(s). *Chem Comm*. **2016**;52:5045–5048.
- [9] Gavel PK, Dev D, Parmar HS, et al. Investigations of peptide-based biocompatible injectable shape-memory hydrogels: differential biological effects on bacterial and human blood cells. *ACS Appl Mater Interfaces*. **2018**;10:10729–10740.
- [10] Gavel PK, Parmar HS, Tripathi V, et al. Investigations of anti-inflammatory activity of a peptide-based hydrogel using rat air pouch model. *ACS Appl Mater Interfaces*. **2019**;10:2849–2859.
- [11] Tiwari P, Basu A, Sahu S, et al. An auxin-tyrosine derivative based biocompatible supergelator: a template for fabrication of nanoparticles for sustained release of model drugs. *New J Chem*. **2018**;42:4915–4922.
- [12] Tiwari P, Rajagopalan R, Moin M, et al. Can self-assembling smart amino acid conjugate hydrogel nanoparticles (HNPs) function as vehicles for drug delivery? *New J Chem*. **2017**;41:308–315.
- [13] Tiwari P, Verma R, Basu A, et al. Proteolysis-resistant self-assembled-amino acid dipeptide-based biocompatible hydrogels as drug delivery vehicle. *Chem Sel*. **2017**;2:6623–6631.
- [14] Fichman G, Gazit E. Self-assembly of short peptides to form hydrogels: design of building blocks, physical properties and technological applications. *Acta Biomaterialia*. **2015**;10:1671–1682.
- [15] Das AK, Collins R, Ulijn RV. Exploiting enzymatic (reversed) hydrolysis in directed self-assembly of peptide nanostructures. *Small*. **2008**;4:279–287.
- [16] Du X, Zhou J, Shi J, et al. Supramolecular hydrogelators and hydrogels: from soft matter to molecular biomaterials. *Chem Rev*. **2015**;115:13165–13307.
- [17] Siegemund G, Schwertfeger W, Feiring A, et al. *Organic Ullmann's encyclopedia of industrial chemistry* Wiley-VCH. Weinheim: Wiley Intersciences Germany; **2005**.
- [18] Aigueperse J, Mollard P, Devilliers D, et al. *Inorganic Ullmann (ed.), encyclopedia of industrial chemistry* Wiley-VCH. Weinheim: Wiley Intersciences Germany; **2005**.
- [19] Bondi A. Van der Waals volumes and radii. *J Phys Chem*. **1964**;68:441–451.
- [20] Stabel A, Dasaradhi L, Hagan DO, et al. Scanning tunneling microscopy imaging of single fluorine atom substitution in stearic acid. *Langmuir*. **1995**;11:1427–1430.
- [21] Booth H, Grindlev TB, Khedhair KA. The anomeric and exo-anomeric effects in 2-methoxytetrahydropyran. *Chem Comm*. **1982**;8:1047–1048.
- [22] Zhou P, Zou J, Tian F, et al. Fluorine bonding — how does it work in protein–ligand interactions? *J Chem Inf Model*. **2009**;49:2344–2355.
- [23] Bustamante E, Pedersen PL. High aerobic glycolysis of rat hepatoma cells in culture: role of mitochondrial hexokinase. *Proc Natl Acad Sci U S A*. **1977**;74:3735–3739.
- [24] Greenwood NN, Earnshaw A. *Chemistry of the elements*. Butterworth Heinemann; **1988**. USA: Elsevier. ISBN 978-0-7506-3365-9.
- [25] Centers for Disease Control and Prevention. Recommendations for using fluoride to prevent and control dental caries in the United States. *MMWR Recommendations Rep*. **2001**;50:1–42.
- [26] Pizzo G, Piscopo MR, Pizzo I, et al. Designing with natural materials. *Clin Oral Invest*. **2007**;11:189–193.
- [27] Emsley J. *Nature's building blocks: an A-Z guide to the elements*. USA: Elsevier, Oxford University Press. ISBN: 9780199605637. 178. **2011**.
- [28] Swinson J. Fluorine - A vital element in the medicine chest. *Pharma Chem*. **2005**;4:26–27.
- [29] Sharma A, Goswami S, Rajagopalan R, et al. Supramolecular Heterogeneity in  $\beta$ -turn forming synthetic peptides nucleated by isomers of fluorinated phenylalanine and Aib as corner residues. *Supramol Chem*. **2015**;27:669–678.
- [30] Sharma A, Tiwari P, DuttKonar A. The dominant role of sidechains in nucleation of double helical organization in synthetic peptides. *J Mol Struct*. **2018**;1161:44–54.
- [31] Wu FY, Hsu SM, Cheng H, et al. The effect of fluorine on supramolecular hydrogelation of 4-fluorobenzyl-capped diphenylalanine. *New J Chem*. **2015**;39:4240–4243.
- [32] Wu C, Zheng Z, Guo Y, et al. Fluorine substitution enhances the self-assembling ability of hydrogelators. *Nanoscale*. **2017**;9:11429–11433.
- [33] Ryan DM, Anderson SB, Nilsson BL. The influence of side-chain halogenation on the self-assembly and hydrogelation of Fmoc-phenylalanine derivatives. *Soft Matter*. **2010**;6:3220–3231.
- [34] Rizvi SAA, Saleh AM. Applications of nanoparticle systems in drug delivery technology. *Saudi Pharm J*. **2018**;26:64–70.
- [35] Sharma Gangele A, Goswami S, Bar A, et al. Can side chain interactions nucleate supramolecular heterogeneity in synthetic tripeptides? *Cryst Growth Des*. **2016**;16:2130–2139.

- [36] DuttKonar A. The unique crystallographic signature of a  $\beta$ -turn mimic nucleated by *N*-Methylated Phenylalanine and Aib as corner residue: conformational and self-assembly studies. *CrystEngComm*. **2013**;15:10569–10578.
- [37] DuttKonar A. *m*ABA inserted supramolecular triple helix formation in the solid state in synthetic tripeptides containing  $\beta$ -cyano alanine and Aib as corner residues. *Cryst Eng Comm*. **2012**;14:6689–6694.
- [38] DuttKonar A. Can a single pyridine dicarboxylic acid ample enough to nucleate supramolecular double helices in enantiomeric pseudo peptides? *CrystEngComm*. **2013**;15:2466–2473.
- [39] Gaussian 09, Revision A. 1. Frisch MJ, Trucks GW, Schlegel HB. et al. Gaussian, Inc.: Wallingford CT; **2009**
- [40] Mehra R, Tiwari P, Basu A, et al. In search of bioinspired hydrogels from amphiphilic peptides for sustained release of anticancer drugs. *New J Chem*. **2019**;43: 11666.
- [41] Mehra R, Basu A, Christmann R, et al. Mechanoresponsive, proteolytically stable and biocompatible supergelators from ultra short enantiomeric peptides with sustained drug release propensity. *New J Chem*. **2020**;44:6346–6354.
- [42] Tiwari P, Basu A, Vij A, et al. Rationally designed bioinspired - Amino valeric acid based hydrogel: one shot solution for drug delivery and effluent management. *ChemistrySelect*. **2019**;4:6896–6905.
- [43] Mahler A, Reches M, Cohen S, et al. Rigid, self-assembled hydrogel composed of a modified aromatic dipeptide. *Adv Mater*. **2006**;18:1365–1370.
- [44] Mutter M, Maser F, Altmann KH, et al. Sequence-dependence of secondary structure formation: conformational studies of host–guest peptides in  $\alpha$ -helix and  $\beta$ -structure supporting media. *Biopolymers*. **1985**;24:1057–1074.
- [45] Moretto V, Crisma M, Bonora GM, et al. Comparison of the effect of five guest residues on the beta-sheet conformation of host (L-val) $_n$  oligopeptides. *Macromolecules*. **1989**;22:2939–2944.
- [46] Han J, Zhao D, Li D, et al. Polymer-based nanomaterials and applications for vaccines and drugs. *Polymers*. **2018**;10:31–45.
- [47] Singh R, Lillard JW. Nanoparticle-based targeted drug delivery. *Exp Mol Pathol*. **2009**;86:215–223.
- [48] Ischakov R, Abramovich LA, Buzhansky L, et al. Peptide-based hydrogel nanoparticles as effective drug delivery agents. *Bioorg Med Chem Lett*. **2013**;21:3517–3522.
- [49] Feng SS, Zeng WT, Lim YT, et al. Vitamin E TPGS-emulsified poly(lactic-co-glycolic acid) nanoparticles for cardiovascular restenosis treatment. *Nanomedicine*. **2007**;2:333–344.
- [50] Galvao TLP, Rocha IM, Ribeiro de Silva MDC, et al. Is uracil aromatic? The enthalpies of hydrogenation in the gaseous and crystalline phases and in aqueous solution, as tools to obtain an answer. *J Phy Chem A*. **2013**;117:5826–5836.